fluids

MDPI

Article

Investigation of the Mass Transfer Ratio in a Bubble Column Operated with Various Organic Liquids and Mixtures Under Ambient Conditions †

Stoyan Nedeltchev

Institute of Chemical Engineering, Polish Academy of Sciences, Baltycka Str. 5, 44-100 Gliwice, Poland; sned@iich.gliwice.pl

† Presented as a poster at the MMPE 2025 Symposium (8–11 September 2025) in Matsue (Japan).

Abstract

In this work, for the first time, the dependence of the mass transfer (MT) ratio (k_La coefficient to overall gas holdup) as a function of the superficial gas velocity U_G in seven organic liquids was studied. The volumetric liquid-phase MT coefficients k_La were recorded (by means of a polarographic oxygen electrode) in a bubble column (0.095 m in ID) equipped with a single tube (∅3.0 mm in ID) as a gas sparger. It was found that the MT ratio decreases monotonically through all main flow regimes. Both the constant and the exponent of the empirical correlation between the MT ratio and U_G were analyzed, and it was found that they depended in a complicated fashion on the Schmidt number, Sc. In three different regions of the *Sc* number, potential new correlations were discussed. The main conclusion from this work is that the MT ratio is not constant in the heterogeneous regime as reported previously by other researchers. In the case of four binary mixtures between benzene and cyclohexane, it was also found that the MT ratio decreased monotonically as a function of the superficial gas velocity, U_G. The effects of both liquid viscosity and surface tension on the MT ratio were also investigated.

Keywords: bubble columns; mass transfer coefficients; mass transfer ratio; monotonically decreasing trendline

1. Introduction

Bubble columns (BCs) are the most frequently used gas–liquid contactors in various industries (chemical, biochemical, petroleum, metallurgical, etc.). They are used for absorption, oxidation, chlorination, alkylation, polymerization, esterification, hydrogenation, bioreaction, fermentation, methanol synthesis and Fischer–Tropsch synthesis (coal liquefaction to produce fuels), wastewater treatment, etc. The main advantages of BCs are associated with their excellent mass transfer (MT) and heat transfer performance as well as their easy maintenance and occupation of limited space. The complex characteristics of the gas–liquid flow are interconnected with both MT and heat transfer processes in BCs. In order to design and optimize BCs, it is necessary to predict their MT efficiency. The occurrence of a chemical reaction could alter both the physical and chemical properties of the phases and then affect the bubble size, gas holdup and MT coefficient.

Various factors have an impact on the MT performance of BCs, including the operating conditions (superficial gas velocity, temperature, pressure, etc.), fluid properties (density, viscosity), reactor structure, size and bed aspect ratio. There is a crucial influence of the

Check for updates

Academic Editor: Wenning Zhou

Received: 4 January 2026
Revised: 30 January 2026
Accepted: 2 February 2026
Published: 4 February 2026

Copyright: © 2026 by the author. Licensee MDPI, Basel, Switzerland. This article is an open access article distributed under the terms and conditions of the Creative Commons Attribution (CC BY) license.

nature of the gas–liquid systems and the character of the gas–liquid dispersions on the MT performance of BCs. Obtaining reliable experimental MT data under complex conditions (high pressure and temperature) is a challenge.

Interphase MT characteristics are quantified by the product of liquid-side MT coefficient k_L and gas–liquid interfacial area a. The k_L value characterizes the influence of the surrounding liquid flow field on the rising bubbles, while the a value inherently represents the system's hydrodynamics and MT behavior.

The approaches for modeling gas–liquid MT for two-phase flows should consider not only molecular diffusion but also the film's motion, which causes convection. The internal flow also intensifies the MT. When the internal circulation currents increase, the interfacial surface renewal accelerates significantly, leading to an increase in the MT rate.

The bubble shape is one of the most important parameters in bubble dynamics, which affects both the gas–liquid interfacial area and the MT rate. As the bubble diameter and gas velocity increase, the bubble shape changes from spherical to ellipsoidal. The bubble aspect ratio serves as a reflection of the bubble shape. For the successful prediction of the MT coefficients, the mobility of the bubble surface is also an important factor. According to Calderbank and Moo-Young [1], bubbles with diameters greater than 3.5 mm behave like fluid particles with a mobile surface in water.

The two most famous MT models are the two-film model [2] and the penetration model [3]. According to the film model, the steady-state molecular transfer controls the region between the films, whereas the penetration theory assumes that the transfer process is unsteady and the convective diffusion controls the MT region. However, these two major MT models have not considered the effect of the eddy diffusion.

The Higbie penetration model [3] states that the fluid elements are transported to the interface by means of convection. In a period called contact (exposure) time, the fluid elements stay at the interface, and during that time, they are likely to share matter (mass) with the gas bubbles by means of molecular diffusion. By convection, they move away from the interface and transmit the matter accumulated in the surrounding liquid. It is assumed that all fluid elements have the same contact time. The latter can be expressed in different ways based on the mean bubble diameter or the bubble length and height.

Batchelor [4] has assumed that the large energy-containing eddies control the MT in turbulent fields. The author has developed a quasi-steady large-eddy model. Later, Lamont and Scott [5] extended this model to include a wider range of eddy sizes in fully developed turbulent fields. These authors assumed that large energy-containing eddies control the MT process in turbulent fields, and thus they have improved the model of Fortescue and Pearson [6].

The effects of bubble shape and bubble swarm on MT should be exhaustively studied. Recently an important research work about these effects has been published by Wang et al. [7]. The authors have developed a new MT model for prediction of the liquid-phase MT coefficient considering both the effects of bubble deformation and the bubble swarm. Wang et al. [7] have also investigated the MT characteristics across different zones of BCs operated under various hydrodynamic regimes. This work is very useful considering the previous difficulties in comprehensively understanding the local MT variations in BCs. The previous MT models proposed in the past decades have not been systematically compared. In many MT models, it was assumed that the bubble shape was spherical, although the bubble shape maps were implying the formation of ellipsoidal bubbles. The assumption of a spherical bubble shape is not plausible since the larger bubbles deform as they rise [7].

1.1. Main MT Correlations

The main MT correlations for prediction of the volumetric liquid-phase MT coefficient k_La have been well summarized in the review articles of Deckwer and Schumpe [8] and Leonard et al. [9]. These correlations are very important since they allow us to calculate the MT time ($1/k_La$), which takes part in every scale-up methodology. The k_La coefficient takes part in important dimensionless scale-up parameters such as Sherwood, Stanton, Damköhler and Schmidt numbers.

Akita and Yoshida [10] have developed an MT correlation that considers the influence of bubble size on the MT coefficient. Hughmark [11] developed an MT correlation (more applicable to the heterogeneous flow regime) based on the bubble rise velocity. It is worth noting that Hughmark's model overlooks the effects of turbulence on MT, which in turn leads to an underestimation of the MT coefficient. Colombet et al. [12] developed an MT correlation based on the gas volume fraction. It was underscored that the correlation is especially effective at U_G values beyond 0.08 m/s since the bubble swarm effect becomes more pronounced. Jordan and Schumpe [13] developed an MT correlation, which is effective not only at ambient pressure but also at elevated pressures.

Nedeltchev et al. [14] developed a new MT correlation based on a correction (due to a bubble shape variation) to the penetration model [3]. The latter needs a correction factor since it is extremely focused on molecular diffusion and neglects the impact of turbulence on the MT dynamics. Deckwer [15] has proposed a new definition of the gas–liquid contact time based on both the length and velocity of the micro eddies.

It is noteworthy that the research group of Morsi [16] has developed a universal MT correlation valid for both gas–liquid and slurry BCs.

1.2. MT Ratio (k_La-to-ε_G)

The two most important parameters for the BC operation are the overall gas holdup ε_G and the volumetric liquid-phase mass transfer coefficient k_La. Vermeer and Krishna [17] and later Vandu and Krishna [18] have found that the ratio of k_La to ε_G (called MT ratio in this work) is constant and equal to 0.48 s^{-1} in the heterogeneous flow regime, i.e., at superficial gas velocities U_G higher than 0.08 m/s. This ratio is also independent of the column diameter. At lower U_G values, the authors [17] argue that the MT ratio drops from 0.8 s^{-1} down to 0.5 s^{-1}. The MT ratio represents the volumetric liquid-phase MT coefficient per unit volume of bubbles [18]. Vandu and Krishna [18] interpreted the constancy of the MT ratio as the independence of the effective bubble diameter on the U_G. The results of Jordan and Schumpe [13] have also confirmed these findings.

2. Experimental Setup

The volumetric liquid-phase MT coefficients k_La were measured by means of dynamic oxygen absorption method [19]. The BC (0.095 m in ID) was equipped with a single tube of ∅3.0 mm in ID. Initially, the available oxygen in the liquid was completely desorbed by nitrogen. The oxygen fugacity was measured by means of a polarographic oxygen electrode (WTW EO 90) inserted horizontally at half of the dispersion height.

In the case of absorption runs, under the assumption of complete liquid mixing, the time-dependent readings of the electrode (in arbitrary units (a.u.)) have been used to extract the k_La coefficient:

$$\ln(C_{E,sat} - C_E) = -(k_La/(1 - \varepsilon_G)) + const \quad (1)$$

where $C_{E,sat}$ is the saturation concentration. In the case of desorption runs, the governing equation was presented in Öztürk et al. [19]. The k_La coefficients were measured three times and the mean values were used further in the analysis. The experimental error was always within ±5.0%. The k_La coefficient was measured in the fully developed region of the bubble

bed, and since perfect liquid mixing was assumed, the measured k_La value was considered valid for the entire bubble bed. That is why it is related to the overall gas holdup, which is also an MT parameter.

The clear liquid height L_0 was set at 0.85 m. The overall gas holdup ε_G was estimated from the measured aerated liquid height L by means of a ruler attached to the column wall: $\varepsilon_G = (L - L_0)/L$.

The MT ratios (k_La-to-overall gas holdup) were measured in seven organic liquids (cf. Table 1) and four organic mixtures between benzene and cyclohexane (cf. Table 1b). The experimental error in the measurements of the physicochemical properties was always within ±5.0%. Standard devices (viscometer, tensiometer and pycnometer) for the measurement of these properties were used.

Table 1. (a) Physicochemical properties of the organic liquids studied. (b) Physicochemical properties of the mixtures between benzene and cyclohexane.

(**a**)					
Organic Liquid	**Density [kg/m^3]**	**Viscosity [Pa s]**	**Surface Tension [N/m]**	**Diffusivity [m^2/s]**	**Schmidt No. [–]**
Acetone	790	0.327×10^{-3}	23.10×10^{-3}	5.85×10^{-9}	70.756
Benzene	879	0.653×10^{-3}	28.70×10^{-3}	3.46×10^{-9}	214.708
Cyclohexane	778	0.977×10^{-3}	24.80×10^{-3}	3.29×10^{-9}	381.697
Ethylacetate	900	0.461×10^{-3}	23.50×10^{-3}	3.46×10^{-9}	148.041
Ethylbenzene	867	0.669×10^{-3}	28.60×10^{-3}	2.94×10^{-9}	262.458
Ligroin	729	0.538×10^{-3}	21.40×10^{-3}	3.29×10^{-9}	224.315
Methanol	790	0.586×10^{-3}	22.20×10^{-3}	3.81×10^{-9}	194.691
(**b**)					
Mixture of Benzene	**Density [kg/m^3]**	**Viscosity [Pa s]**	**Surface Tension [N/m]**	**Diffusivity [m^2/s]**	**Schmidt No. [–]**
+cyclohexane 6.7%	865	0.634×10^{-3}	27.60×10^{-3}	3.61×10^{-9}	202.976
+cyclohexane 13.4%	854	0.628×10^{-3}	26.90×10^{-3}	3.63×10^{-9}	202.356
+cyclohexane 78.5%	797	0.772×10^{-3}	24.90×10^{-3}	3.16×10^{-9}	306.142
+cyclohexane 90.0%	787	0.858×10^{-3}	24.90×10^{-3}	2.95×10^{-9}	369.816

The mixtures of benzene and cyclohexane studied in this work are common in the petrochemical industry, particularly as products of benzene hydrogenation to create cyclohexane, often forming close-boiling, non-ideal mixtures that require specialized separation techniques. They are miscible in all proportions in the liquid phase, with positive excess molar volumes. These mixtures are produced via catalytic hydrogenation of benzene and must be separated to obtain pure cyclohexane. Because they form azeotropic mixtures (close boiling points), separating them requires methods like extractive distillation or adsorption.

3. Results and Discussion

3.1. Dependence of the MT Ratio on the Superficial Gas Velocity in Organic Liquids

Figure 1 shows that in the case of the air–acetone system, the MT ratio exhibits a decreasing trend as a function of the superficial gas velocity U_G. In the figure is also shown the power-law correlation between both parameters: MT ratio = $AU_G{}^b$. The exponent b (−0.104) of U_G is relatively low.

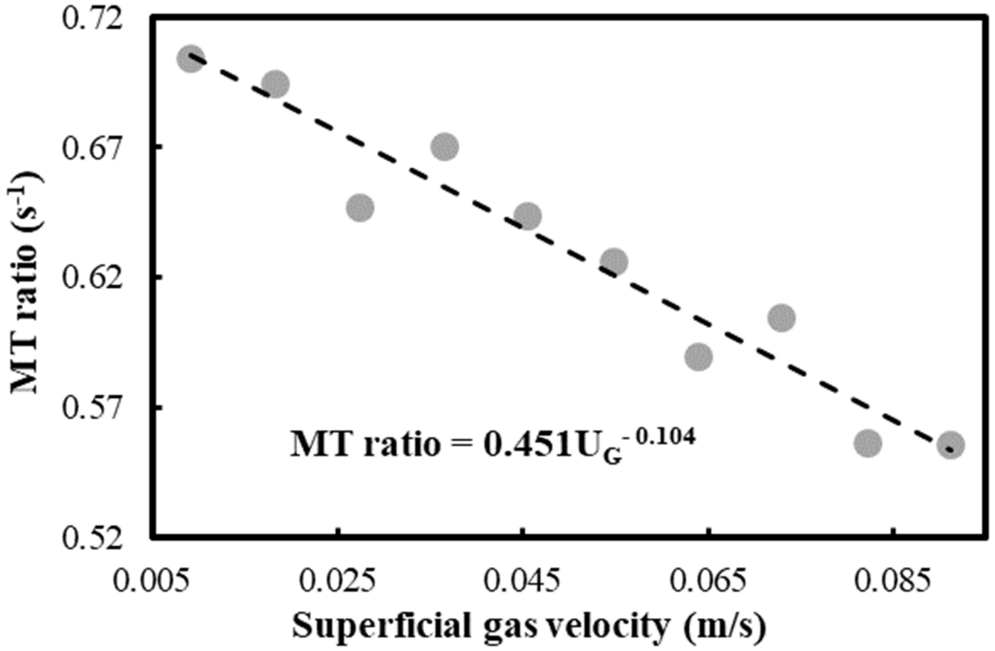


Figure 1. Profile of the MT ratio as a function of U_G in the air–acetone system.

Figure 2 shows that the main transition velocity (end of the homogeneous regime) can be identified at U_G = 0.046 m/s based on the variation in the bubble rise velocity as a function of the superficial gas velocity U_G. When the results in Figures 1 and 2 are compared, it becomes clear that the main flow regime change does not affect the profile of the MT ratio.

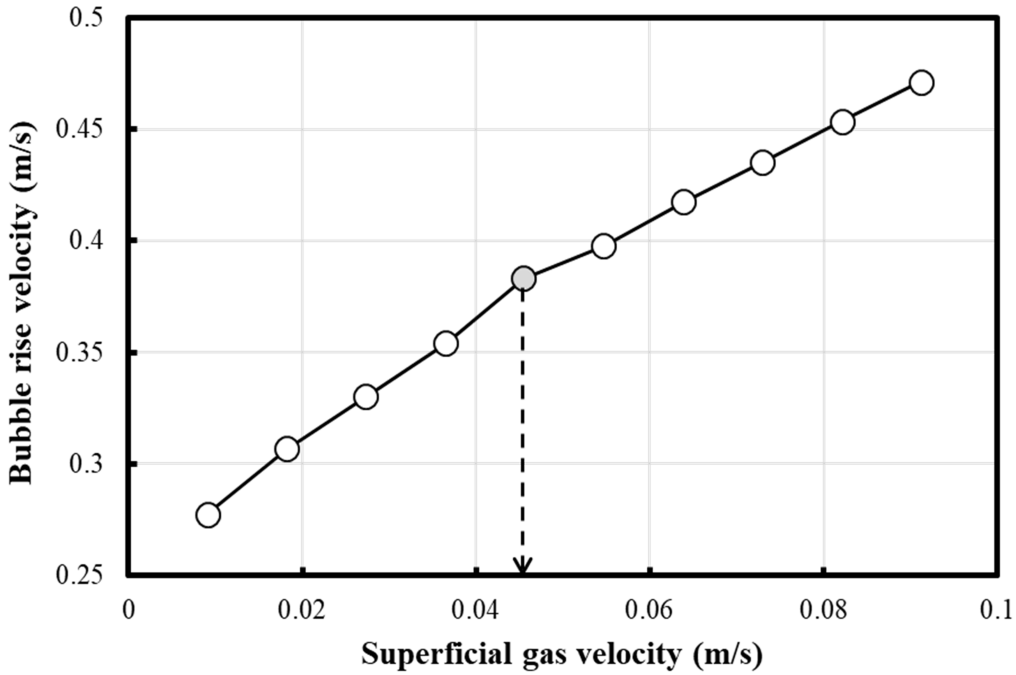


Figure 2. Variation of the bubble rise velocity as a function of superficial gas velocity U_G in the air-acetone system.

Figure 3 shows that in the case of the air–benzene system, the MT ratio exhibits also a decreasing trend as a function of the superficial gas velocity U_G. In the figure, the empirical correlation between both parameters is also shown. The exponent b (−0.147)

of U_G is somewhat lower than the one for acetone. The constant A (0.351) is also lower. It is noteworthy that this value is close to the reciprocal value (3/8 = 0.375) of the drag coefficient C_D in a turbulent flow surrounding the bubble [20].

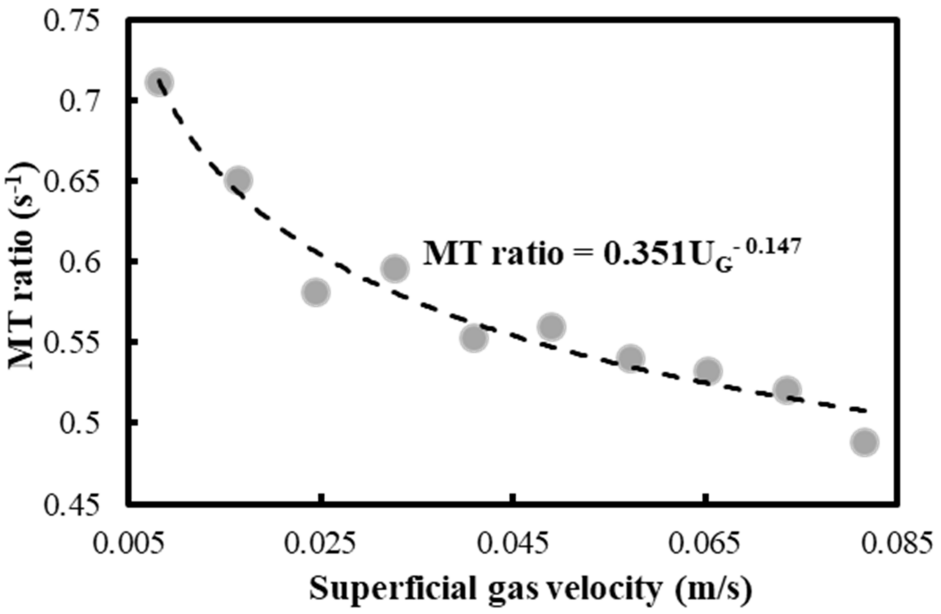


Figure 3. Profile of the MT ratio as a function of U_G in the air–benzene system.

Figure 4 shows that in the case of the air–cyclohexane system, the MT ratio also exhibits a decreasing trend as a function of the superficial gas velocity U_G. In the figure, the power-law correlation between both parameters is also shown. The exponent b (−0.200) of U_G is somewhat lower than the one for benzene and twice lower compared to the case of acetone. The constant (0.215) is also lower than the other two cases.

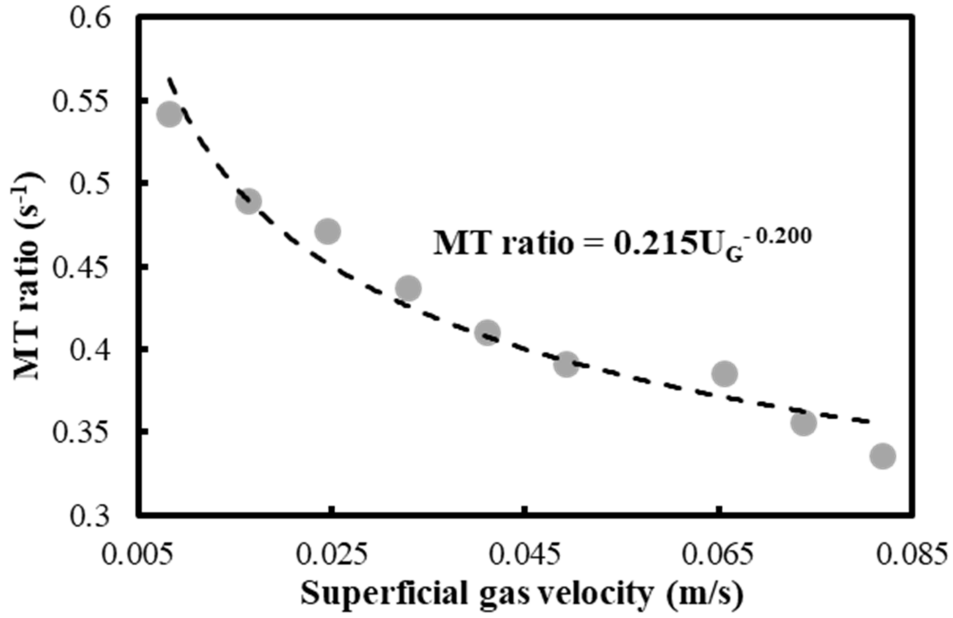


Figure 4. Profile of the MT ratio as a function of U_G in the air–cyclohexane system.

Figure 5 shows that in the case of the air–ethylacetate system, the MT ratio also exhibits a decreasing trend as a function of the superficial gas velocity U_G. In the figure, the power-law correlation between both parameters is also shown. The exponent b (−0.079) of U_G is

the lowest as compared to the other cases. The constant A (0.462) is very close to the one for the air–acetone system.

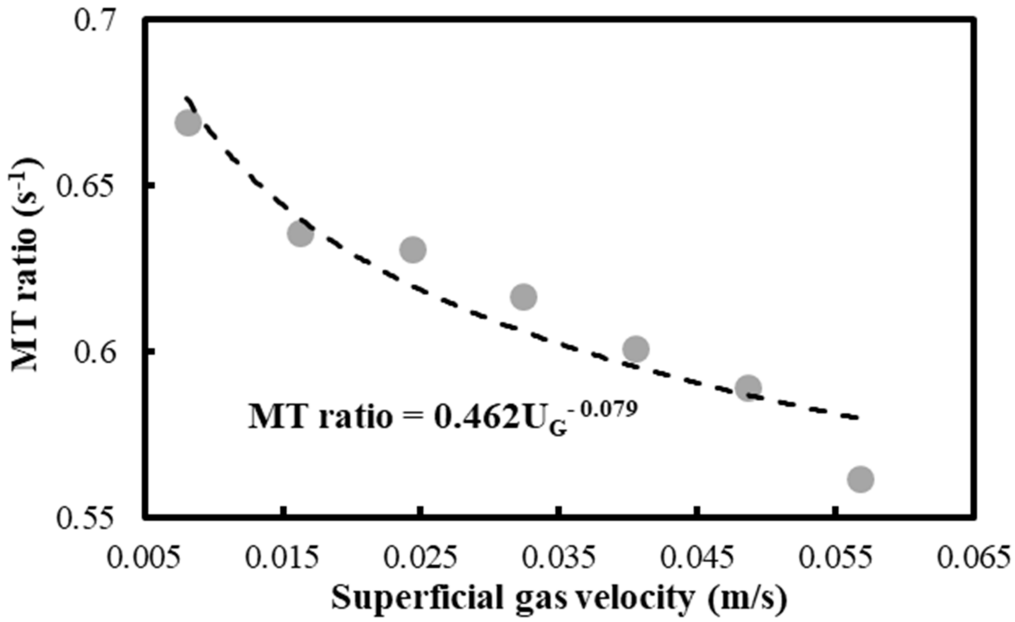


Figure 5. Profile of the MT ratio as a function of U_G in the air–ethylacetate system.

Figure 6 shows that in the case of the air–ethylbenzene system, the MT ratio also exhibits a decreasing trend as a function of the superficial gas velocity U_G. In the figure, the empirical correlation between both parameters is also shown. The exponent b (−0.085) of U_G is very close to the one (−0.079) shown in Figure 5. The constant A (0.445) is also very close to the one (0.462) for the air–ethylacetate system.

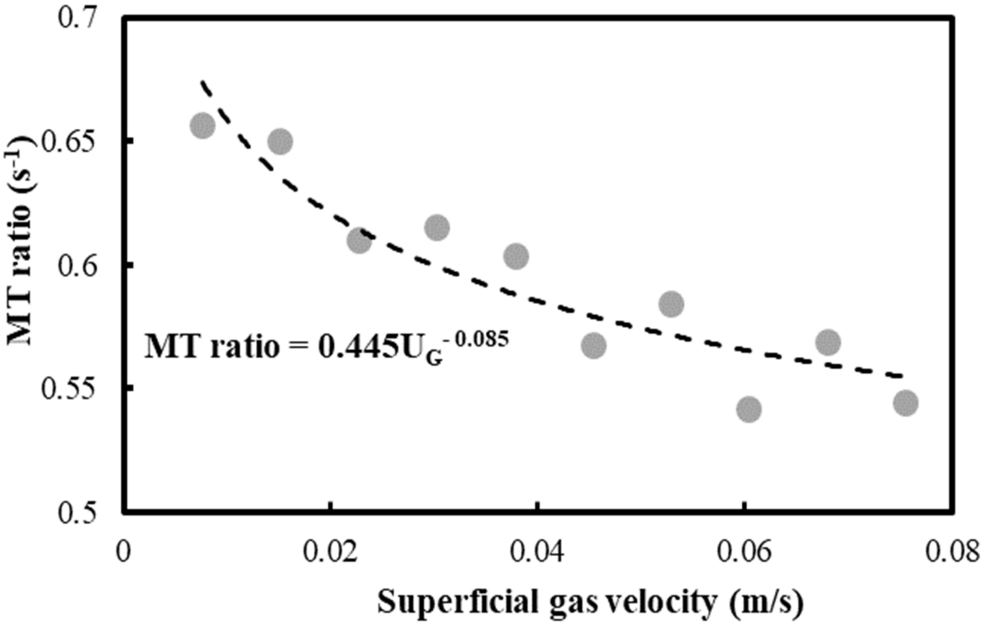


Figure 6. Profile of the MT ratio as a function of U_G in the air–ethylbenzene system.

Figure 7 shows that in the case of the air–methanol system, the MT ratio also exhibits a decreasing trend as a function of the superficial gas velocity U_G. In the figure, the power-law correlation between both parameters is also shown. Both the exponent b (−0.117) of U_G and the constant A (0.440) are very close to the one for the air–acetone system.

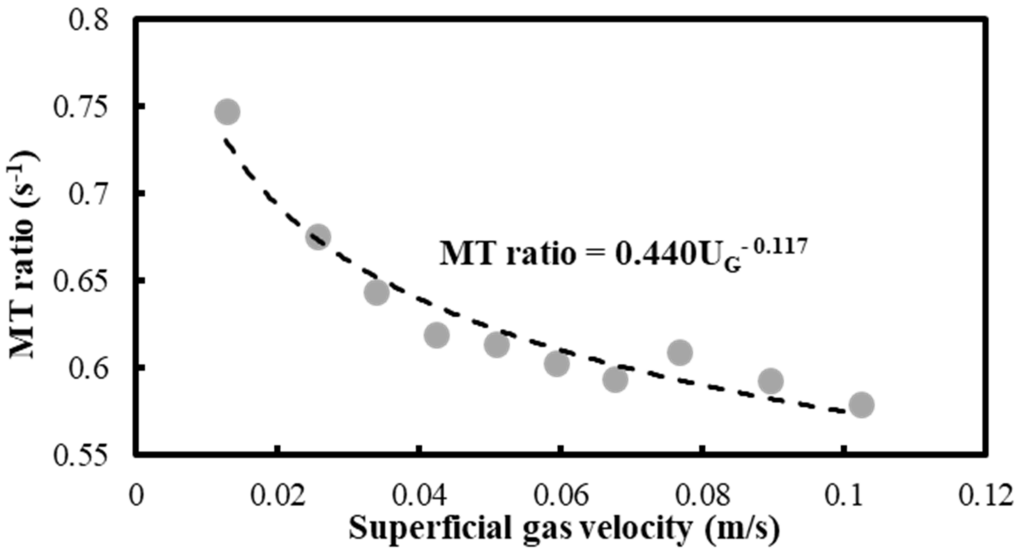


Figure 7. Profile of the MT ratio as a function of U_G in the air–methanol system.

Figure 8 shows the monotonical decrease of the MT ratio in the air–ligroin system. The constant A and the exponent b are the lowest.

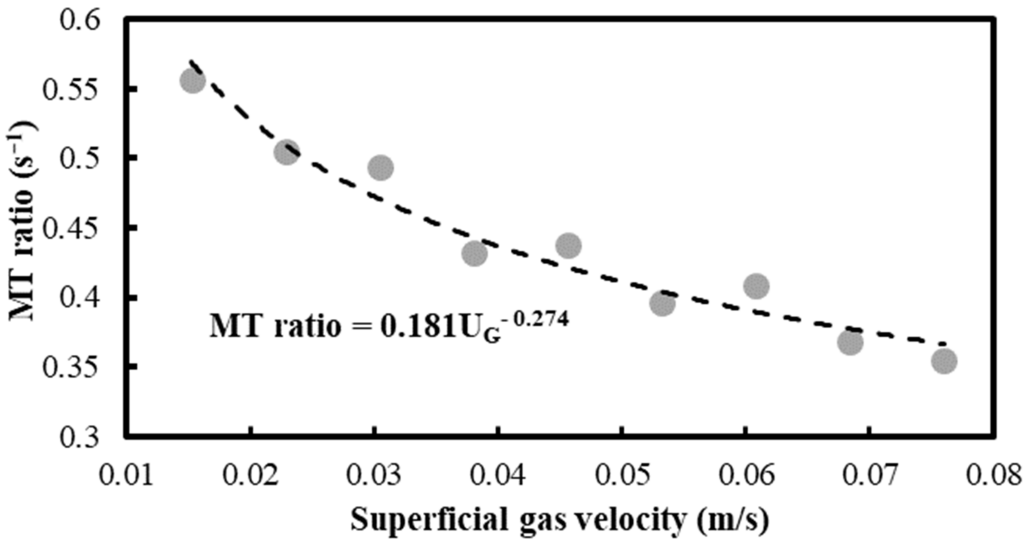


Figure 8. Profile of the MT ratio as a function of U_G in the air–ligroin system.

3.2. Dependence of the MT Ratio on the Superficial Gas Velocity in Liquid Mixtures

When mixtures of benzene and cyclohexane are aerated with an air, the dependence of the MT ratio on the U_G is similar to the cases with organic liquids. Figure 9 shows that in the case of a mixture of benzene with 6.7% cyclohexane, the MT ratio decreases monotonically through all main flow regimes. The empirical correlation is characterized with a constant A equal to 0.342 and an exponent b equal to −0.164. This result is very close to the air–benzene case (cf. Figure 3). The exponent is somewhat lower, whereas the constant is again close to the inverse value of the drag coefficient C_D (8/3) under turbulent conditions.

When the concentration of cyclohexane in the mixture increases to 13.4%, the constant A remains practically the same (cf. Figure 10) and very close to the inverse value of C_D but the exponent b increases somewhat to −0.113.

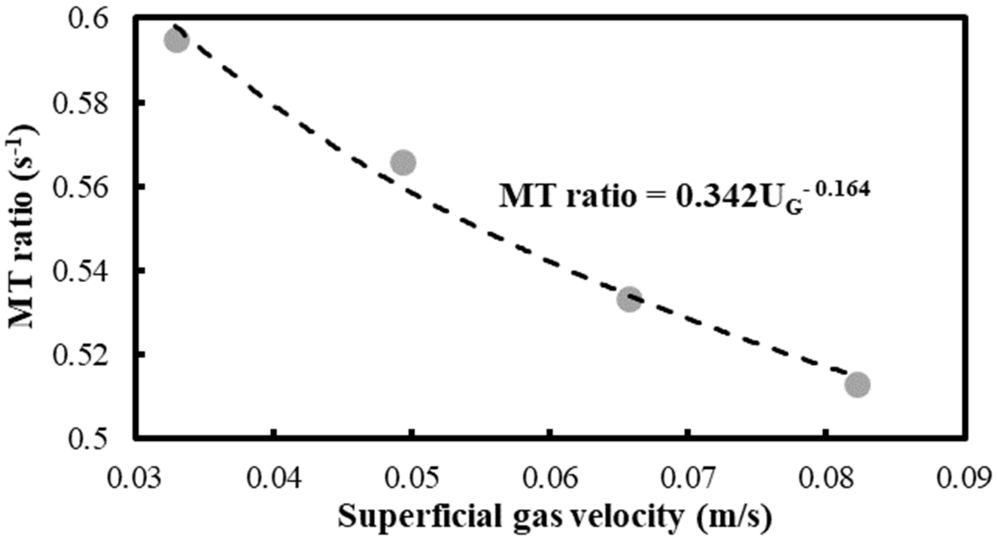


Figure 9. Profile of the MT ratio as a function of U_G in the 6.7% benzene–cyclohexane mixture.

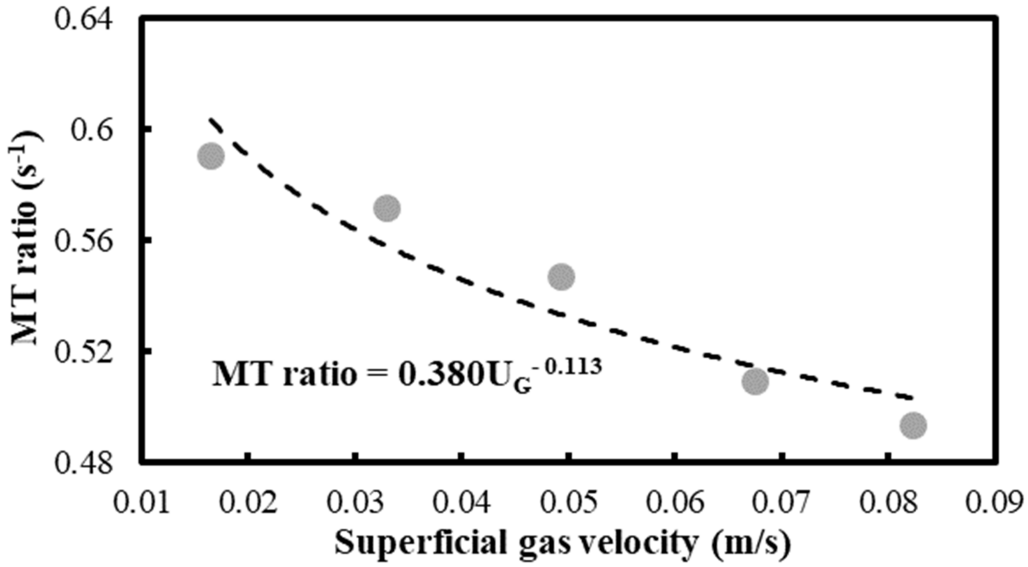


Figure 10. Profile of the MT ratio as a function of U_G in the 13.4% benzene–cyclohexane mixture.

When the concentration of cyclohexane increases to 78.5%, the constant A decreases somewhat down to 0.362 (cf. Figure 11), but it is still close to the characteristic value of 0.375 ($1/C_D$). The exponent b takes the value of -0.105, which is practically the same as the one in the case of Figure 10.

When the contents of the cyclohexane in the mixture increase to 90.0% (cf. Figure 12), the constant A drops down to 0.322, which is already a sensible deviation from the value of 0.375 ($1/C_D$). The exponent b decreases somewhat to -0.127.

3.3. Dependence of the Fitting Parameters on the Schmidt Number

It was found that for both the constant A and the exponent b, there are three separate regions where they could be correlated differently to the Schmidt number Sc. The latter represents the ratio of kinematic viscosity to molecular diffusivity. Figure 13a,b show that universal correlations for A and b with respect to the Sc number are not possible. In the profiles of both A and b, the first region spans for Sc numbers from 50 to 148, the second region spans from 148 to 224, and the third region covers Sc numbers from 224 to 382. A well-pronounced minimum in the profiles of both parameters occurs at an Sc value of 224.

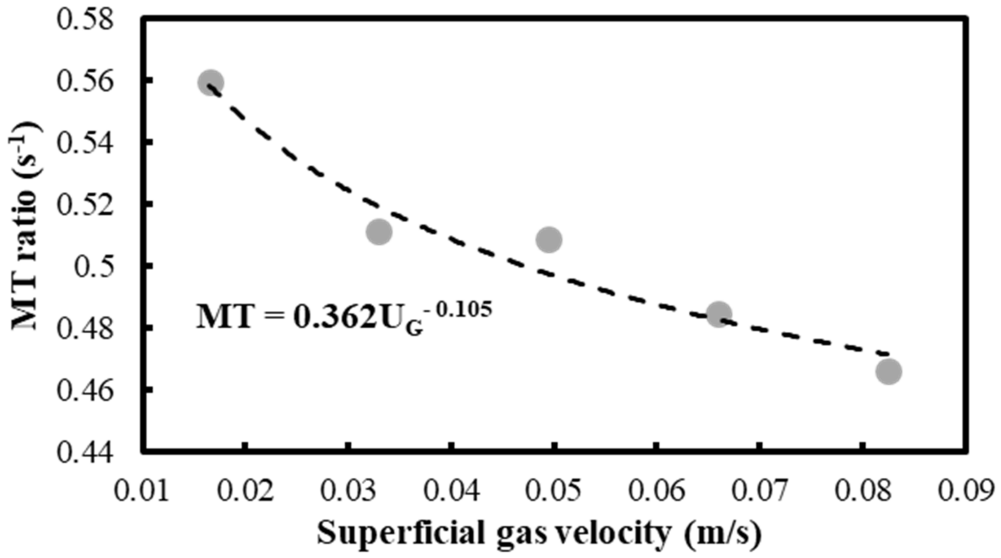


Figure 11. Profile of the MT ratio as a function of U_G in the 78.5% benzene–cyclohexane mixture.

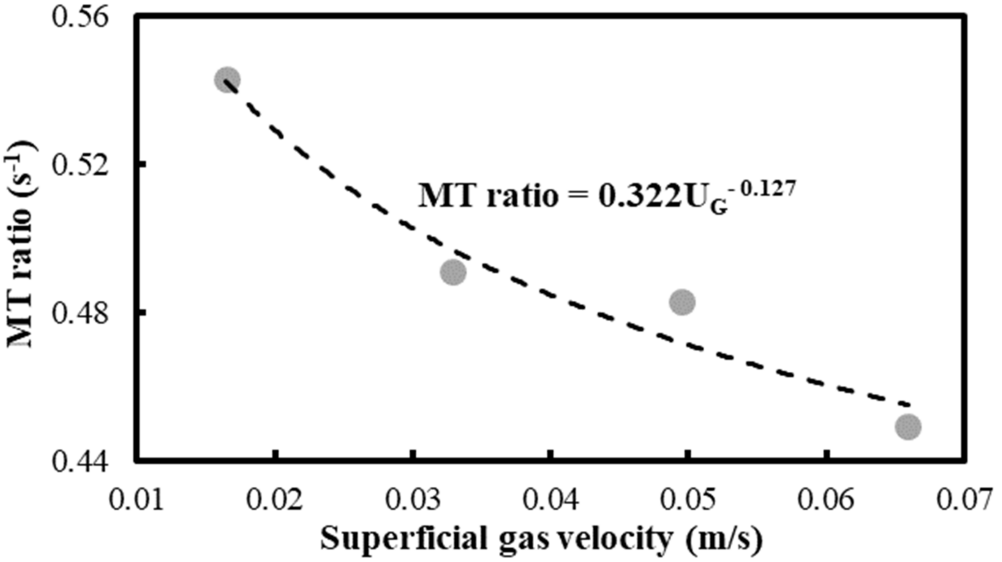


Figure 12. Profile of the MT ratio as a function of U_G in the 90.0% benzene–cyclohexane mixture.

The k_La coefficient slightly depends (exponent = 0.17) on the column diameter (Akita and Yoshida [21]). On the other hand, the overall gas holdup does not depend on the column diameter [21]. So, based on these considerations, it is expected that the MT ratio will increase only slightly in larger bubble columns.

3.4. Dependence of the MT Ratio on the Liquid Viscosity

Figure 14a shows that the MT ratio depends on the liquid viscosity in a complicated way in organic liquids aerated with air at a U_G value of 0.0082 m/s. At a liquid viscosity of 0.00054 Pas (ligroin), the MT ratio exhibits a well-pronounced minimum. This range of liquid viscosity should be avoided since the MT is the lowest and thus less efficient. At liquid viscosities beyond 0.00065 Pas, the MT ratio decreases monotonically. The same findings are observed at U_G = 0.0163 m/s (cf. Figure 14b).

3.5. Dependence of the MT Ratio on the Surface Tension

There is also a local minimum in the dependence of the MT ratio on the surface tension. In the case of cyclohexane (surface tension = 0.0248 N/m), there is a well-pronounced local minimum in the MT ratio values. Such a condition should be avoided since the MT process is ineffective. Beyond this critical surface tension, the MT ratio tends to increase. These findings are demonstrated at two U_G values: at U_G = 0.0082 m/s (Figure 15a) and at U_G = 0.0163 m/s (Figure 15b).

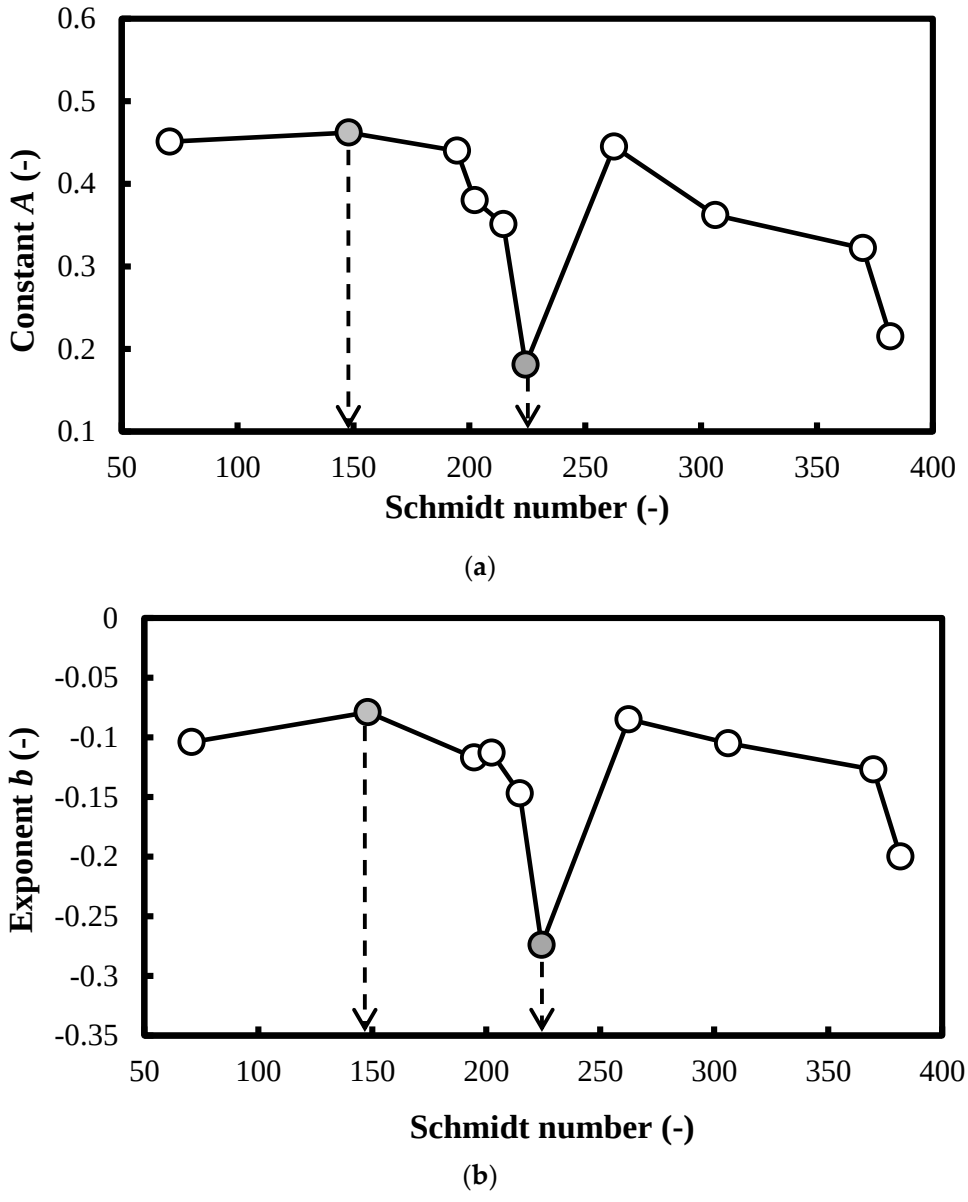
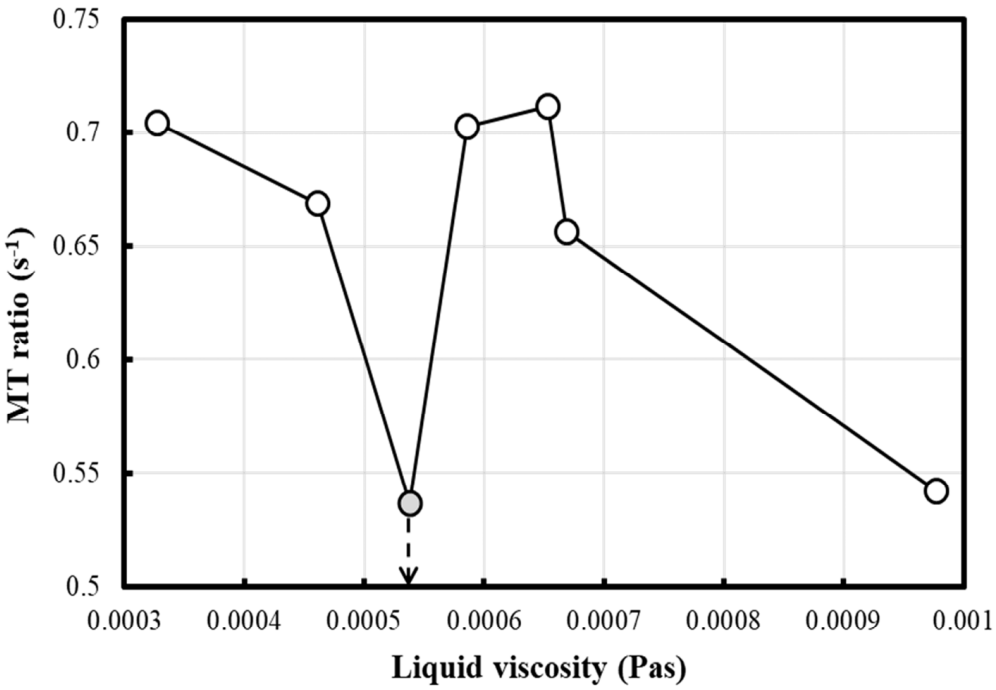
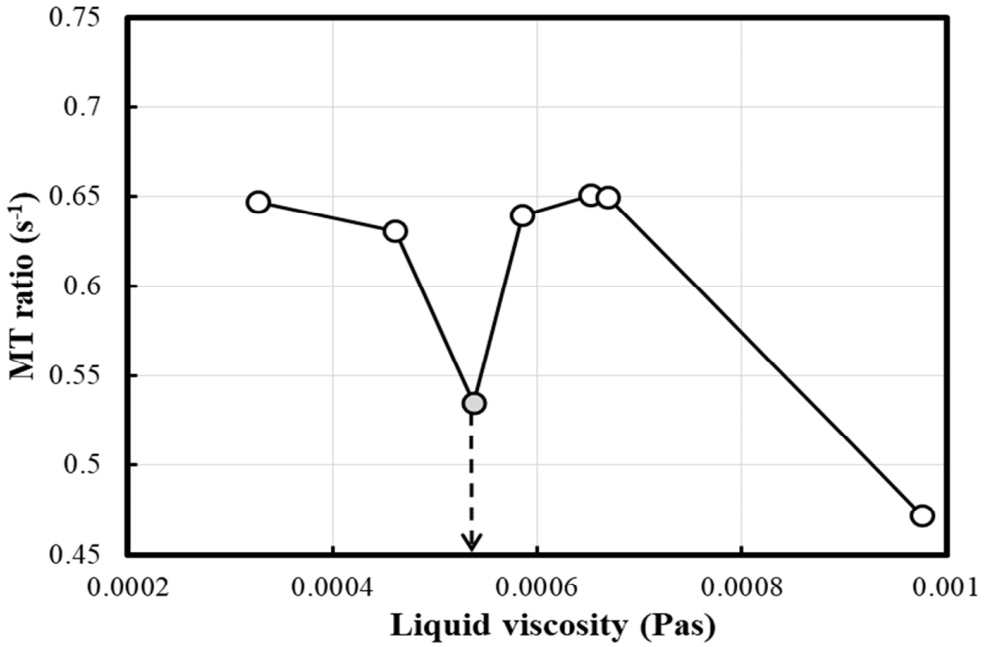


Figure 13. (**a**) Profile of the constant *A* as a function of the Schmidt number *Sc*. (**b**) Profile of the exponent *b* as a function of the Schmidt number *Sc*.



(**a**)



(**b**)

Figure 14. (**a**) Profile of the MT ratio as a function of the liquid viscosity at U_G = 0.0082 m/s. (**b**) Profile of the MT ratio as a function of the liquid viscosity at U_G = 0.0163 m/s.

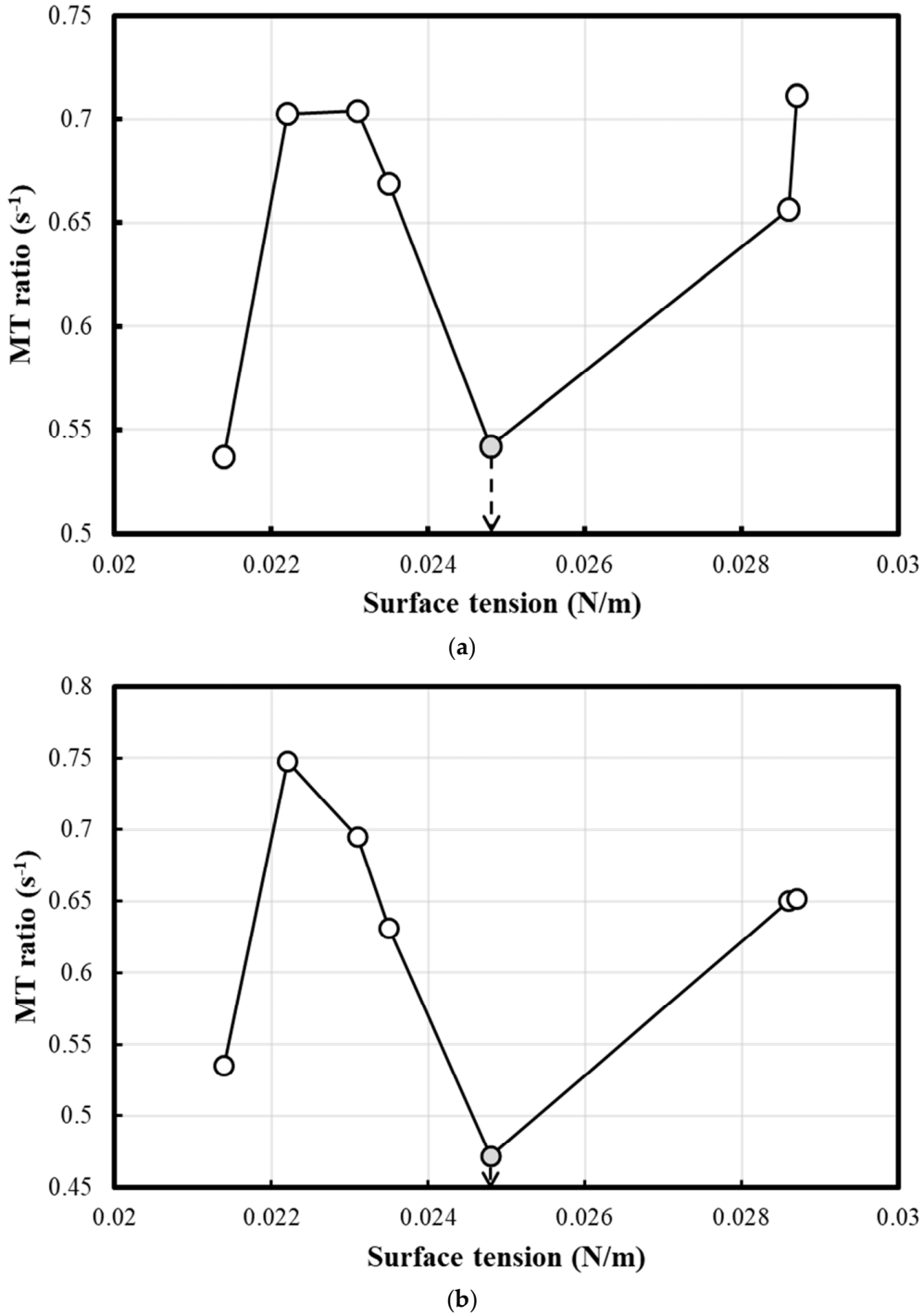


Figure 15. (**a**) Profile of the MT ratio as a function of the surface tension at U_G = 0.0082 m/s. (**b**) Profile of the MT ratio as a function of the surface tension at U_G = 0.0162 m/s.

4. Conclusions

In this work, the dependence of the mass transfer (MT) ratio (k_La coefficient-to-gas holdup) on the superficial gas velocity U_G in a bubble column (0.095 m in ID) operated with seven different organic liquids has been studied. It was found that in all hydrodynamic regimes, the MT ratio decreases monotonically as a function of U_G. In such a way, it has been proven that the previous results of some researchers are not generally valid and the MT ratio is not constant in the heterogeneous flow regime.

Empirical correlations between the MT ratio and U_G have been developed. Both the constant A and the exponent b have been correlated to the Schmidt number Sc, and it has been found that there are three regions in which these parameters could be correlated in different ways to the Sc number. In other words, generally valid empirical correlations between the parameters A and b and the Sc number are not feasible.

In the case of four mixtures between benzene and cyclohexane, it has also been found that the MT ratio decreases monotonically as a function of the superficial gas velocity U_G.

Finally, the MT values (in seven organic liquids) as a function of both liquid viscosity and surface tension have been investigated. It has been found that in both cases, there is a well-pronounced local minimum. Beyond this critical value, the MT ratio decreases in the case of liquid viscosity, whereas it tends to increase in the case of the surface tension.

Funding: This research received no external funding.

Institutional Review Board Statement: Not applicable.

Informed Consent Statement: Not applicable.

Data Availability Statement: The mass transfer data can be obtained directly from the author.

Conflicts of Interest: The author declares no conflicts of interest.

Abbreviations

BC	bubble column
ID	inner diameter
MT	mass transfer

Nomenclature

a	gas–liquid interfacial area	m^{-1}
A	constant in the MT correlation	–
b	exponent in the MT correlation	–
C_D	drag coefficient in a turbulent flow	–
C_E	concentration of dissolved oxygen	a.u.
$C_{E,sat}$	liquid concentration at saturation	a.u.
D_L	molecular diffusivity	m^2/s
k_L	liquid-phase MT coefficient	m/s
k_La	volumetric liquid-phase MT coeff.	s^{-1}
L_0	clear liquid height	m
L	aerated liquid height	m
U_G	superficial gas velocity	m/s
Dimensionless number		
Sc	Schmidt number	–
Greek letters		
ε_G	overall gas holdup	–

References

1. Calderbank, P.H.; Moo-Young, M.B. The continuous phase heat and mass-transfer properties of dispersions. *Chem. Eng. Sci.* **1961**, *16*, 39–54. [CrossRef]
2. Lewis, W.K.; Whitman, W.G. Principles of gas absorption. *Ind. Eng. Chem.* **1924**, *16*, 1215–1220. [CrossRef]
3. Higbie, R. The rate of absorption of a pure gas into a still liquid during short periods of exposure. *Trans. Am. Inst. Chem.* **1935**, *31*, 365–389.
4. Batchelor, G.K. *An Introduction to Fluid Dynamics*; Cambridge University Press: Cambridge, UK, 1967.
5. Lamont, J.C.; Scott, D.S. An eddy cell model of mass transfer into the surface of a turbulent liquid. *AIChE J.* **1970**, *16*, 513–519. [CrossRef]
6. Fortescue, G.E.; Pearson, J.R.A. On gas absorption into a turbulent liquid. *Chem. Eng. Sci.* **1967**, *22*, 1163–1176. [CrossRef]

7. Wang, X.-Q.; Wen, Z.-Q.; Zhang, X.-B.; Li, H.; Luo, Z.-H. Numerical simulation of mass transfer characteristics of gas-liquid bubble columns and an improved mass transfer model. *Ind. Eng. Chem. Res.* **2024**, *63*, 8473–8486. [CrossRef]
8. Deckwer, W.-D.; Schumpe, A. Improved tools for bubble column reactor design and scale-up. *Chem. Eng. Sci.* **1993**, *48*, 889–911. [CrossRef]
9. Leonard, C.; Ferrasse, J.-H.; Boutin, O.; Lefevre, S.; Viand, A. Bubble column reactors for high pressures and high temperatures operation. *Chem. Eng. Res. Des.* **2015**, *100*, 391–421. [CrossRef]
10. Akita, K.; Yoshida, F. Bubble size, interfacial area, and liquid-phase mass transfer coefficient in bubble columns. *Ind. Eng. Chem. Proc. Des. Dev.* **1974**, *13*, 84–91. [CrossRef]
11. Hughmark, G.A. Holdup and mass transfer in bubble columns. *Ind. Eng. Chem. Proc. Des. Dev.* **1967**, *6*, 218–220. [CrossRef]
12. Colombet, D.; Legendre, D.; Cockx, A.; Guiraud, P.; Risso, F.; Daniel, C.; Galinat, S. Experimental study of mass transfer in a dense bubble swarm. *Chem. Eng. Sci.* **2011**, *66*, 3432–3440. [CrossRef]
13. Jordan, U.; Schumpe, A. The gas density effect on mass transfer in bubble columns with organic liquids. *Chem. Eng. Sci.* **2001**, *56*, 6267–6272. [CrossRef]
14. Nedeltchev, S.; Jordan, U.; Schumpe, A. Correction of the penetration theory based on mass-transfer data from bubble columns operated in the homogeneous regime under high pressure. *Chem. Eng. Sci.* **2007**, *62*, 6263–6273. [CrossRef]
15. Deckwer, W.-D. On the mechanism of heat transfer in bubble column reactors. *Chem. Eng. Sci.* **1980**, *35*, 1341–1346. [CrossRef]
16. Lemoine, R.; Behkish, A.; Sehabiague, L.; Heintz, Y.J.; Oukaci, R.; Morsi, B.I. An algorithm for predicting the hydrodynamic and mass transfer parameters in bubble column and slurry bubble column reactors. *Fuel Proc. Techn.* **2008**, *89*, 322–343. [CrossRef]
17. Vermeer, D.J.; Krishna, R. Hydrodynamics and mass transfer inn bubble columns operating in the churn-turbulent regime. *Ind. Eng. Chem. Process Des. Dev.* **1981**, *20*, 475–482. [CrossRef]
18. Vandu, C.O.; Krishna, R. Influence of scale on the volumetric mass transfer coefficients in bubble columns. *Chem. Eng. Proc.* **2004**, *43*, 575–579. [CrossRef]
19. Öztürk, S.S.; Schumpe, A.; Deckwer, W.-D. Organic liquids in a bubble column: Holdups and mass transfer coefficients. *AIChE J.* **1987**, *33*, 1473–1480. [CrossRef]
20. Miller, D.N. Scale-up of agitated vessels gas-liquid mass transfer. *AIChE J.* **1974**, *20*, 445–453. [CrossRef]
21. Akita, K.; Yoshida, F. Gas hold-up and volumetric mass transfer coefficients in bubble columns. *Ind. Eng. Chem. Process Des. Dev.* **1973**, *12*, 76–80. [CrossRef]

Disclaimer/Publisher's Note: The statements, opinions and data contained in all publications are solely those of the individual author(s) and contributor(s) and not of MDPI and/or the editor(s). MDPI and/or the editor(s) disclaim responsibility for any injury to people or property resulting from any ideas, methods, instructions or products referred to in the content.